Design of a Synchronous Reluctance Machine for Recuperation of a Truck Trailer

1st Zeller Tobias
Institute of Electrical Engineering
Karlsruhe Institute of Technology
Karlsruhe, Germany
t.zeller@kit.edu

2nd Baumhäckel David
Institute of Electrical Engineering
Karlsruhe Institute of Technology
Karlsruhe, Germany

3rd Doppelbauer Martin
Institute of Electrical Engineering
Karlsruhe Institute of Technology
Karlsruhe, Germany
martin.doppelbauer@kit.edu

***Abstract*—While most attention on reducing greenhouse gas emissions has been focused towards the passenger vehicle sector, the electrification of utility vehicles is also steadily progressing. This development is being driven by the resolutions to limit global warming to 1.5°C above pre-industrial levels, which were determined at the Paris and Glasgow climate conferences in 2015 and 2021 [1], [2]. In urban environments, the use of trucks with refrigeration systems to transport fresh products is common. These refrigeration systems are generally powered by an additional diesel engine contained within the trailer. This paper presents an alternative solution for energy generation using recuperation via a generator located in the truck trailer axle. A complete system analysis of the vehicle axle, transmission, and generator was performed. From this, a tool chain was derived and implemented to perform a multi-criteria optimization of the overall system. The tool chain performs an optimization of the aforementioned components of the system to determine the best utilized generator based on a selected driving cycle. The generator itself can also be optimized, with different rotor topologies and the perfect combination ratio of slots to pole pairs being worked out.**

***Index Terms*—Design of a synchronous reluctance machine, synchronous reluctance machine for recuperation, recuperation of truck trailer**

I. Introduction

In recent years, the introduction of electric drive systems has not only made progress in the passenger car sector, new EU-regulations also drive the electrification trend in the heavy vehicle sector [1], [2]. With the introduction of the "European Green Deal", road traffic emissions must be reduced across the various vehicle sectors [3]. In addition to the obvious approach of replacing the drive unit with one that is battery or hydrogen powered, there is also the opportunity to replace the auxiliary power supply units (APUs), which are traditionally powered by diesel engines. These APUs power a variety of different components, such as pumps or refrigerators [3], [4]. Depending on the size and legal requirements of the truck, the dimensions, and the amount of energy supplied by the APU will differ. This work focuses on the refrigeration unit of a semi-truck-trailer. To replace the diesel engine, an alternative power source must be found. As already proven in passenger cars, energy recovery by recuperation can increase efficiency significantly. The proposed concept connects a generator with a gearbox to the axle of a truck trailer and uses the braking torque to feed energy into a battery powering the refrigeration unit.

Similar approaches already exist, such as the "TRAKr-project" produced by SAF-Holland and Advanced Electric Machines (AEM) [5], [6]. AEM offers a synRM with a continuous power of $P_{\mathrm{cont.}} = 20\,\mathrm{kW}$ and a maximum torque of $M_{\mathrm{peak}} = 90\,\mathrm{N\,m}$ in combination with a gearbox and a rigid axle produced by SAF-Holland. BPW Bergische Achsen and Thermo King LLC have also developed a new axle module. The BPW ePower module generates energy while the trailer is in motion to supply cooling units power during temperature-controlled transports [7], [8]. Benevelli Srl follows a slightly different approach. They also produce electric drive axles, with powers ranging from $0.5-30\,\mathrm{kW}$, but the generator can be an asynchronous machine, synchronous interior permanent motor, Permanent magnet synchronous motor or an axial flux machine depending on the application [9].

However, it is evident that none of the variants or approaches presented above have been designed as a complete system and rely only on connecting individually designed components (such as gearbox, rigid axel, or the generator). A consideration of the overall system and thus the complete performance and efficiency chain has yet to be considered. In this paper, we present a design proposal for a synchronous reluctance machine (synRM) in combination with a gearbox where recuperation is used to generate energy to replace the diesel powered APU unit. The schematic structure of the system is shown in Fig. 1.

II. Boundary Conditions

Various boundary conditions must be defined for the design of a recuperation generator. In the following, these are divided into two different sub-areas and explained in detail.

A. Boundary Conditions – Geometry/Mechanical

To achieve the maximum possible strength, an electrical steel sheet with a yield strength of $560\,\mathrm{MPa}$ is used. Reference [10] states that every additional component increases the system weight and leads to additional consumption, while the payload that can be transported decreases. The power density of the generator is the deciding factor in order to ensure maximum payload. Environmental conditions such as

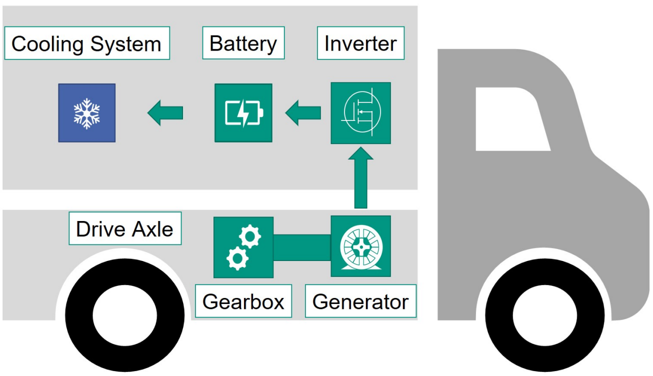

Fig. 1: Schematic structure of the total system

temperature, rain, or humidity playing a subordinate role in the design process.

B. Boundary Conditions – Electrical

The inverter used as an example in this study is an ISC1 12-50-IC developed by SciMo GmbH. It offers a good balance of light weight, high voltage and high current. It supplies a continuous current of $I_{\mathrm{RMS}} = 70\,\mathrm{A}$ and a peak voltage of $U_{\mathrm{DC,peak}} = 800\,\mathrm{V}$ with a weight of approximately $m_{\mathrm{inverter}} = 2.5\,\mathrm{kg}$ [11].

C. Boundary Conditions – Drive

To design an optimal generator, the highest possible efficiency (η) must be achieved in a drive cycle. A typical $26\,\mathrm{t}$ vehicle in distribution transport usually drives with a maximum speed of approximately $80\,\mathrm{km\,h^{-1}}$. A typical working shift of $8-9$h) and route of a truck driver is used for the simulations. The truck drives about $\sim 3\,\mathrm{h}$ and $50\,\mathrm{min}$, then is unloaded and loaded for $\sim 1\,\mathrm{h}$ before driving to the next station. The driving and loading cycle is repeated throughout the day.

This results in a pure driving time of $7\,\mathrm{h}$ and $40\,\mathrm{min}$ (the waiting times at traffic lights in the driving cycle are not extracted) with a $2\,\mathrm{h}$ break for unloading. During unloading and loading, the required energy is taken from the battery. The cooling system, used in this paper, is the "Supra 1250 MT" by Carrier [12] requiring an average power of $9\,\mathrm{kW}$.

III. MODELING

A. Initial Investigation

Using analytical equations, an initial investigation of the final machine was conducted. The equations given in the following are taken from [13]. The inner apparent power of the machine (P_{si}) is defined by the internal voltage (E_h), the current (I), and the number of phases (m):

$$P_{si} = m \cdot E_h \cdot I. \tag{1}$$

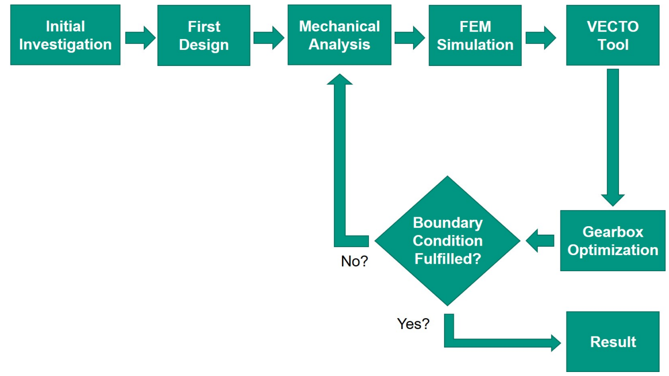

Fig. 2: Flowchart of the generator design process

E_h is determined by the amplitude of the main flux ($\hat{\Phi}_h$), the corresponding number of turns (w), the winding factor (ξ), and the circular frequency (ω):

$$E_h = \frac{1}{\sqrt{(2)}} \cdot \omega \cdot (w\xi) \cdot \hat{\Phi}_h. \tag{2}$$

The main flux in turn can be determined by the flux density ($\hat{B}$), the pole pitch (τ_p), and the active length (l_{fe}) of the machine:

$$\hat{\Phi}_h = \frac{2}{\pi} \cdot \hat{B} \cdot \tau_p \cdot l_{fe}. \tag{3}$$

By varying combinations of the basic machine parameters such as the number of slots (N), the number of pole pairs ($2p$), current, and voltage, as well as many others, a sample design for different machines was produced. The relevant data of the first design can be found in table I. To keep the basic behavior of the different machines the same, the number of slots per pole per phase was kept.

These machines form the basis for subsequent design using Finite-Element-Method (FEM). The design flow chart of the generator is shown in Fig. 2. The "First Designs" from the initial investigation are subsequently checked mechanically for stability, and then examined electromagnetically using "FEM". The resulting machines are rated in their efficiency by the "Vehicle Energy Consumption calculation TOol" (VECTO tool) by the European Commission, followed by an optimization of the "Gearbox". Finally, it was examined whether the "Boundary Conditions" have been fulfilled.

TABLE I: Rough design parameters of different machines

Parameter of First Design	Machine 1	Machine 2	Machine 3
Number of Slots - N (-)	24	36	48
Number of Pole Pairs - $2p$ (-)	2	3	4
Number of Slots per Pole per Phase - q (-)		2	
Bore Diameter - D_{i} (mm)		113	
DC Link Voltage - $U_{\mathrm{DC,peak}}$ (V)		800	
RMS Current - I_{RMS} (A)		70	

B. Automated Machine Calculation

The analytical draft design of the generator is followed by the automated calculation using FEM. Flux® by Altair® is used for the electromagnetic investigation. The initial geometry setting of the machine is chosen with the help of the FluxMotor® program. Diameter based parameters, number of pole pairs, the main rotor topology and stator slot topology can no longer be changed during the simulation run, which is why care must be taken to ensure that the initial geometry settings for these parameters are correct. Afterward, a python file is generated by FluxMotor®, listening all essential machine characteristics is saved in a target folder. In Matlab®, the simulation-specific settings are chosen, in which, for example, the maximum speed, voltage, and current are specified. In addition, the variation parameter range is defined using a "Design of Experiments" study, for more details see Fig. 3). This allows the geometry of the flux barriers of the rotor and the stator slot to be changed. Starting from Matlab® and the FluxMotor® python file, all machine models are modeled in Flux2D®, checked with respect to their geometry and faulty geometries are eliminated. The numerical field calculation is then performed in Flux2D®. The FEM results are imported into Matlab® where a detailed loss calculation and evaluation of the finite element calculation is performed, before displaying the results graphically. The presented procedure has already been described in more detail in [14].

C. Rotor Topology

Flux® offers the possibility to use predefined rotor topologies for a synRM. A sampling of these different topologies are given in Fig. 3. The number of flux barriers is defined by the letter index (A-D). A denotes one flux barrier and D denotes four flux barriers. The different rotor topologies are defined from 1-8. In addition to the parameters for each topology, the number of flux barriers can be modified as well. This creates a variable parameter space of up to 40 different parameters for a single rotor structure. Equivalently, the parameters also apply to other combinations of N and p. It is evident that the parameter space of the individual parameters cannot be chosen to be infinitely large and are partially dependent on each other. Therefore, an analytical tool was developed that detects unfeasible structures (e.g., edges lying on top of each other) and sorts them out even before the FEM calculation.

D. Mechanical Analysis

As soon as the generator rotates and thus store energy in the battery, centrifugal forces are applied on the rotor material and cause stresses. To define the mechanical strength of the topologies and thus, their maximum speed, a mechanical analysis is performed using Ansys® Mechanical (see example result in Fig. 4). As can be seen, the maximum stress doesn't exceed the possible yield strength of $560\,\mathrm{MPa}$ and is therefore suitable for the FEM-Simulation. Due to symmetry conditions in the simulation and the selected boundary conditions, it is sufficient to examine a single pole and extrapolate to the entire rotor. Each calculated machine design and therefore all the different rotor topologies are mechanically examined. A safety factor of 1.2 is assumed. Especially at high speeds and small bridges (see Fig. 3 parameter W and T3), the reluctance machine

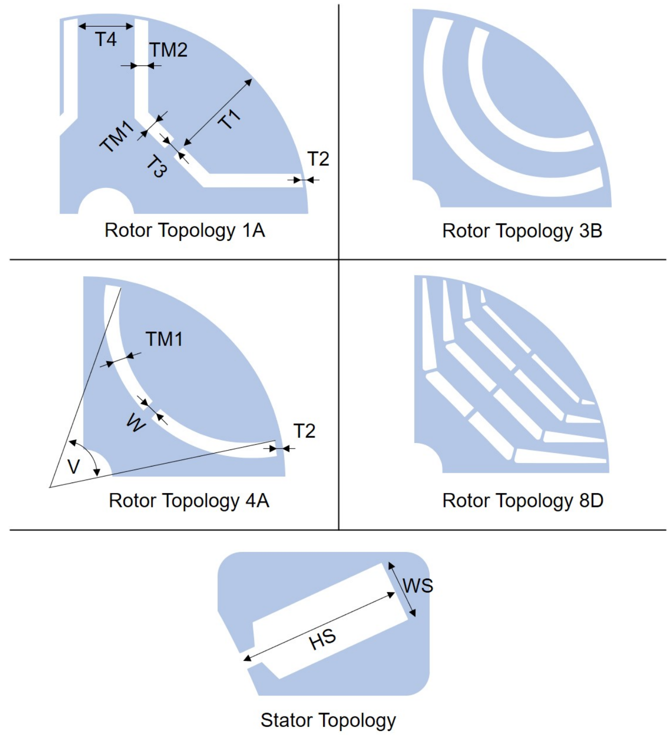

Fig. 3: Example of different rotor topologies with and without parameters, and a range of different flux barriers. As also below, the variation of the stator slot.

shows its electrical strength [15]. Therefore, an electrical sheet with a yield strength of $R_{p0.2} = 560\,\mathrm{MPa}$ is chosen to optimize the endurable stress. Based on all the mechanical analysis, the choice of the best topology depends strongly on the maximum speed. Preliminary investigations indicate that the topology without a center bridge (see Fig. 3 - Topology 3) is optimal up to about $14\,000\,\mathrm{min}^{-1}$. Above this speed, a topology with a center bridge is mechanically more suitable.

E. Drive Cycle and Gearbox Optimization

In order to determine the advantages of the system while driving, it must be defined under which conditions and at which speed sequences the vehicle moves. For this analysis, the VECTO tool by the European Commission is used. VECTO is a software tool developed by the European Union to accurately calculate the energy consumption and CO_2 emissions of heavy-duty vehicles such as trucks. It uses a simulation-based approach that takes into account various factors such as vehicle weight, engine power, aerodynamic drag, and rolling resistance to calculate the fuel consumption and CO_2 emissions of a vehicle under different driving conditions [16]. Various trucks and drive cycles can be selected in the VECTO tool. All of them and the corresponding calculations are based on the WHTC-cycle (World Harmonized Transient Cycle) see [17]. The "Urban Delivery" drive cycle and a "Class 9 Rigid" truck weighing $26\,\mathrm{t}$ running 22.5 inch rims and $315\,\mathrm{mm}$ wide tires featuring

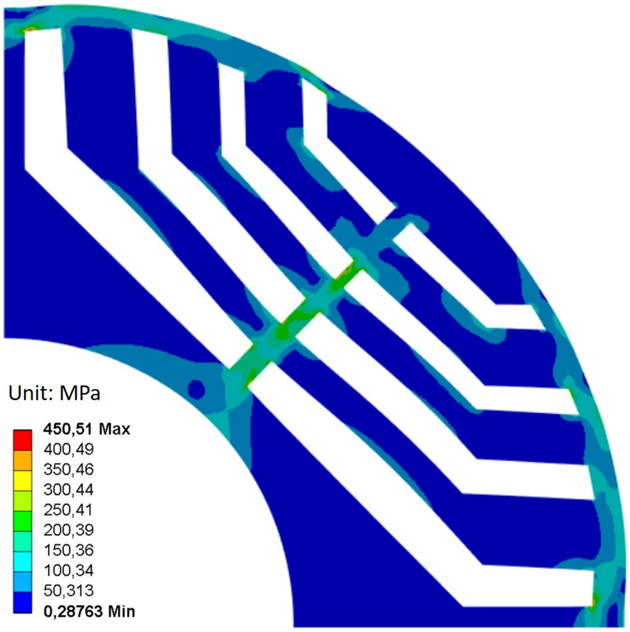

Fig. 4: Representation of a single pole of the maximum von Mises stress in MPa at $12\,000\,\mathrm{min}^{-1}$ of the 2D rotor topology. The deformation has been magnified 50 times for better visualization.

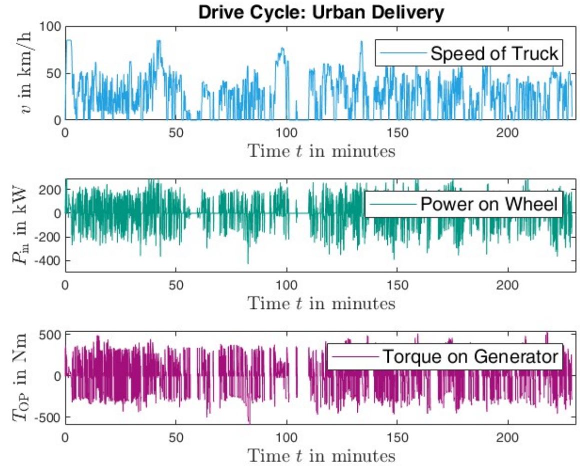

Fig. 5: Drive Cycle ”Urban Delivery” by VECTO with the speed of the truck the power on the wheel and the corresponding torque on the generator with a gear ration $i = 30$.

a height to width ratio of, $70\,\%$ was selected for the design process. The drive cycle is characterized by low maximum speeds and a typical start-stop sequence as used in the urban environment.

The duration of the drive cycle is $\sim 3\,\mathrm{h}$ and $50\,\mathrm{min}$ with several motor and generator segments, see Fig. 5. Since only recuperation is considered in this study, only the operating points that generate negative power at the wheel (also called input power (P_{in})) are used. The input power is calculated by the VECTO-Tool. It depends on what speed the vehicle must reach at which operating point. If the corresponding operating point (required speed) is higher than the current operating point (current speed), the vehicle must accelerate. If the required speed is below the current speed, the vehicle must brake accordingly and thus partially recuperate. In this way, all operating points at which recuperation occures can be determined.

The torque (T_{OP}) applied to the generator is determined by the negative input power, the corresponding angular frequency (ω) and the total gear ratio (i)

$$T_{OP} = \frac{P_{in}}{\omega} \cdot \frac{1}{i} \tag{4}$$

The angular frequency (ω) can be calculated from the velocity (v) and the tire radius (r_{tire}) (see (5)).

$$\omega = \frac{v}{r_{tire}} \tag{5}$$

The torque applied to the generator via the drive train can now be determined. This makes it possible to calculate the total energy fed into the system during recuperation.

Fig. 7 shows the generated power points over the power characteristic curve. A majority of the operating points are clearly above the maximum power characteristic of the calculated machine. These operating points are clipped to the maximum value of the power characteristic curve.

Depending on the overall gear ratio, the operating points shift accordingly to lower torques and higher speeds with higher gear ratio (see Fig. 7 and 8 the blue and orange points). However, since the torque/power and speed curves differ for each machine and the related maxima are at different speeds, a corresponding optimum must be found for each machine. With a pure gear ratio change, the operating points can be shifted to the corresponding maxima of torque and power.

F. *Optimization of Recuperation through the Drive Cycle*

In addition to optimizing the operating points in relation to the torque/speed characteristic and power/speed characteristic, the result of the optimization can also be illustrated in a 3D-plot.

In Fig. 6 a small section of the different machines is given as an example. Simulated is the rotor topology 7D with four flux barriers. The corresponding machine, the gear ratio and the amount of energy that the according machine can recuperate during a drive cycle are plotted.

IV. CONCLUSION

In this paper, a toolchain was developed with the aim of solving an optimization problem within a multi-criteria parameter space consisting of generator design, gear ratio and drive cycle. By applying the flow chart in Fig. 2, first calculations were made to show the function, different machines and gear

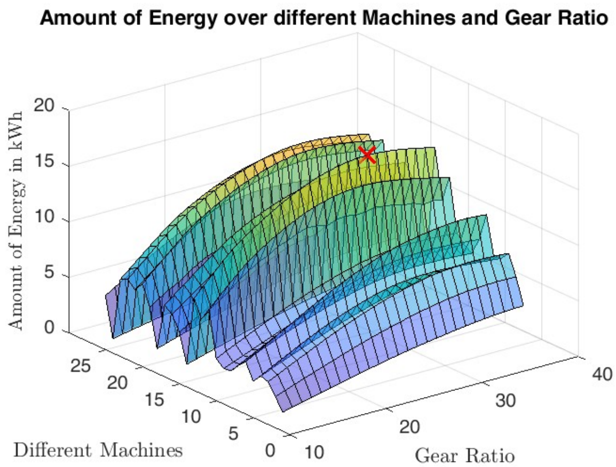

Fig. 6: Example selection of 25 machines plotted against gear ratio and amount of energy that can be generated during one drive cycle.

ratios are obtained, with each satisfing the boundary conditions and thus providing maximum recuperation energy in a drive cycle. Reference [18] and [19] indicate that the machines with a high number of flux barriers (in this paper four), produce the most power and therefore the most energy. With the help of the resulting tool chain, initial parameters could be narrowed down. The results of the mechanical analysis shows that the rotor topology 1D seems to be the most suitable for speeds less than $18\,000\,\mathrm{min}^{-1}$. This can be explained, as the topology 1D has fewer bridges compared to topology 8D, resulting in more electromagnetic flux.

Although the iron losses as well as the AC-losses increase, with rising frequency since they are frequency-dependent (see [15], [13]) it turns out, that the combination of $\frac{N}{p} = \frac{48}{4}$ can generate the highest powers and thus the highest amount of energy during the driving cycle. Since the additional torque gained clearly exceeds these increasing losses, machine 3 recuperates more energy than machines 1 and 2. The power inverter selected in the boundary conditions does not reach the required power, but scaling of the power modules should enable the required current of $95\,\mathrm{A}$.

V. OUTLOOK

As of now, a finalized machine has not been developed. Further investigations regarding different number of turns, currents and voltages, skewing and optimal active length are still pending. Furthermore, in certain situations, it may be beneficial to perform a load point shift on the truck's combustion engine in order to optimize efficiency. For this, further investigations must be conducted with regard to timing, duration and intensity. In addition to the before mentioned factors, further optimization can be carried out with regard to the driving cycle. Currently, only a single drive cycle (Urban-Drive-Cycle) and a single use case have been considered. However, the developed tool chain can be extended to include further driving cycles and use cases like driving profiles of the vehicle fleet operators. It would also be possible to work out specific load profiles (especially in regard to the refrigerated unit) in cooperations with supermarket chains, as no information is currently available on the frequency and time length of the open refrigerated trailer. This introduces additional loss aspects that could not be considered yet. As already mentioned, an optimum of the battery capacity and the corresponding driving cycle must also be determined. Here, data of a vehicle fleet operator could enable the exploration of unknown boundary conditions, such as average traffic jams or unforeseen situations.

REFERENCES

[1] United Nations. (2015) Paris aagreement. [Online]. Available: https://unfccc.int/sites/default/files/english_paris_agreement.pdf

[2] COP26. (2021) Glasgow climate pact. [Online]. Available: https://ukcop26.org/the-glasgow-climate-pact/

[3] I. C. Borbujo, P. G. Pereirinha, M. G. Vega, J. A. Del Valle, and J. C. A. Anton, "Heavy duty transport descarbonization: Legislation and standards for hydrogen and battery electric buses and heavy-duty trucks," in *2021 IEEE Vehicle Power and Propulsion Conference (VPPC)*. IEEE, 2021, pp. 1–6.

[4] Neigel Marx, Daniel Hissel, Fabien Harel, Elodie Pahon, Benoit Courteille, and Frederic Chaillou, "On the design of a hybrid fuel cell - battery genset for a refrigerated semi-trailer truck," in *2018 IEEE Vehicle Power and Propulsion Conference (VPPC)*. IEEE, 2018. [Online]. Available: http://ieeexplore.ieee.org/servlet/opac?punumber=8603846

[5] Editorial staff. (28.07.2021) Saf-holland electric trailer axles undergo (successful) on-road testing. [Online]. Available: https://www.sustainabletruckvan.com/saf-holland-electric-trailer-axles/

[6] S.-H. GmbH, "Saf trakr: Electric axle that is rare earth-free," 22.04.2021. [Online]. Available: https://safholland.com/pt/en/news/article/saf-trakr-electric-axle-that-is-rare-earth-free

[7] BPW Bergische Achsen, "Generating energy on the traile: Bpw epower." [Online]. Available: https://www.bpw.de/fileadmin/user_upload/Service/Downloads/ePower_FLY_BPW_2021_211104-EN.pdf

[8] Steve Banner, "The case for, and against, semi-trailer e-axles," 09.11.2021. [Online]. Available: https://www.transportengineer.org.uk/transport-engineer-features/the-case-for-and-against-semi-trailer-e-axles/242014/

[9] Benevelli Srl, "Electric transaxles: Battery powered axles with power from 0,5 to 30kw," 2022. [Online]. Available: https://www.benevelli-group.com/en/products-for-electric-vehicles-en/electric-transaxles-en.html

[10] Vivek A. Sujan, P.T. Jones and Adam Siekmann, "Heavy duty commercial vehicle platooning energy benefits for conventional and electrified powertrains," 2022 International Conference on Connected Vehicle and Expo (ICCVE. [Online]. Available: https://ieeexplore.ieee.org/stamp/stamp.jsp?tp=&arnumber=9742749

[11] Dr.-Ing. Marc Veigel, "Power electronics and inverter," 05.12.2022. [Online]. Available: https://sci-mo.de/power-electronics/

[12] Carrier Transicold, "Datasheet supra refrigeration," 2022. [Online]. Available: https://www.shareddocs.com/hvac/docs/2000/Public/01/TT_EMEA_SUPRA_ENG.pdf

[13] G. Müller, K. Vogt, and B. Ponick, *Berechnung elektrischer Maschinen*, 6th ed., ser. Elektrische Maschinen / Germar Müller. Weinheim: Wiley-VCH, 2011, vol. Bd. 2.

[14] P. Winzer, "Steigerung von drehmoment und wirkungsgrad bei synchronmaschinen durch nutzung der magnetischen asymmetrie," Ph.D. dissertation, Karlsruher Institut für Technologie (KIT), 2017.

[15] M. Greule, "Frequenzabhängige verluste einer hochdrehenden geschalteten reluktanzmaschine," Ph.D. dissertation, Karlsruher Institut für Technologie (KIT), 2018.

[16] EUROPEAN COMMISSION, "Vecto tool development: Completion of methodology to simulate heavy duty vehicles fuel consumption and co2 emissions," 30.10.2017. [Online]. Available: https://climate.ec.europa.eu/system/files/2017-12/sr7_lot4_final_report_en.pdf

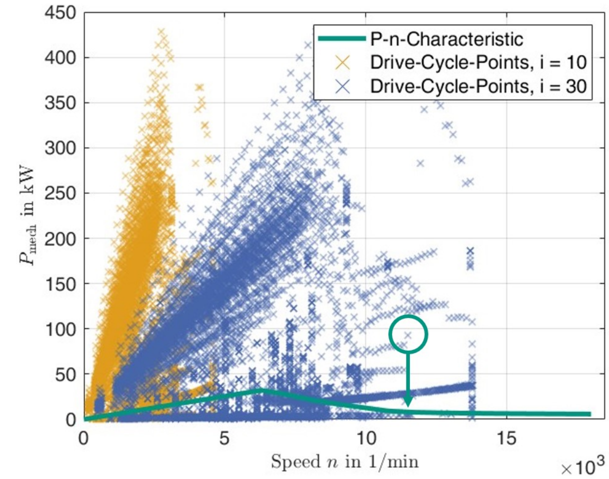

(a) Maximum input power P_{in} accessible on the gearbox

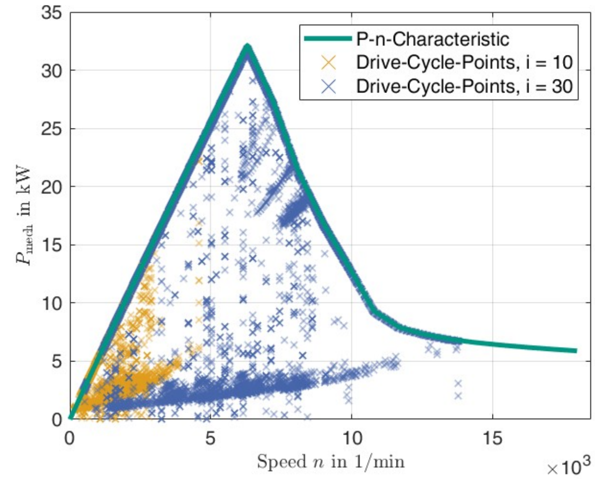

(b) Clipped operating points on the maximum power curve

Fig. 7: Example of different gear ratios and their influence on the operating point shift. As an illustration, an operating point has been marked which is clipped to the maximum power characteristic curve.

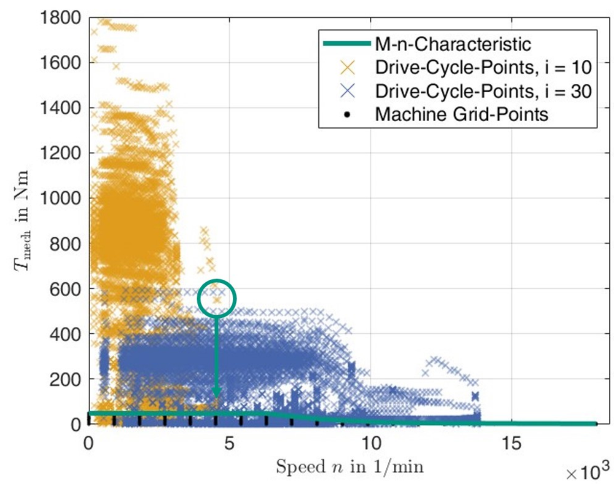

(a) Representation of two different gear ratios and their maximum torque T_{OP} at corresponding speed.

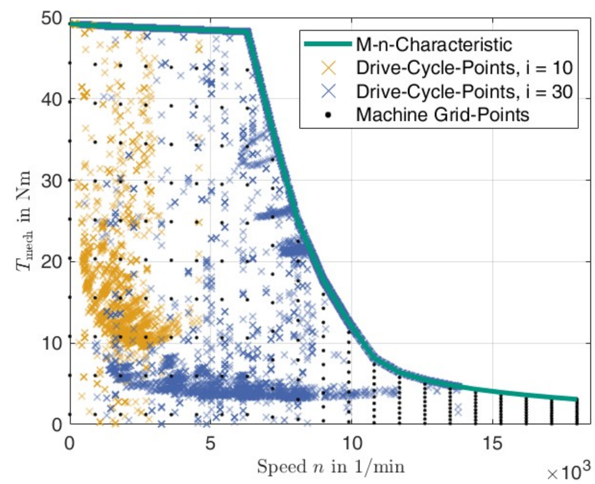

(b) Clipped operating points on the maximum torque curve

Fig. 8: Example of different gear ratios and their influence on the operating point shift. As an illustration, an operating point has been marked which is shifted to the maximum torque characteristic curve.

[17] Monica Tutuianu, Alessandro Marotta, Heinz Steven, Eva Ericsson, Takah Noriyuki Ichikawa, Hajime Ishii, "Development of a world-wide worldwide harmonized light duty driving test cycle (wltc)," The Working Party on Pollution and Energy (GRPE) - 68.

[18] Alfredo Vagati, "Synchronous reluctance electrical motor having a low torque-ripple design," 11.07.1995.

[19] Y. B. Yilmaz and E. Bostanci, "Effects of rotor flux barrier design on torque ripple and high speed performance of synchronous reluctance machines," in *2020 International Conference on Electrical Machines (ICEM)*. IEEE, 2020, pp. 448–454.

VI. Biographies

Tobias Zeller was born in Freiburg, Germany. He received his B.Sc. and M.Sc. degrees in mechanical engineering from the Karlsruhe Institute of Technology (KIT) in 2017 and 2020, respectively. He is currently working towards his Ph.D. degree at the Karlsruhe Institute of Technology (KIT) in the laboratory of hybrid electric vehicles (HEV). His research interests include reluctance machine for recuperation of truck trailer.

David Baumhäckel was born in Villingen-Schwenningen, Germany. He received his B.Sc. and M.Sc. degrees in Electrical engineering and information technology from the Karlsruhe Institute of Technology (KIT) in 2020 and 2022, respectively. He wrote his master's thesis in 2022 at the Institute of Electrical Engineering.

Martin Doppelbauer is full professor since 2011 at the Institute of Electrical Engineering (ETI) at the Karlsruhe Institute of Technology (KIT) in Karlsruhe, Germany. He holds a chair for Hybrid Electric Vehicles. Prior to that, he worked in industry for 15 years, most recently as head of electrical machine development at SEW Eurodrive GmbH in Bruchsal. Martin Doppelbauer is also active in national and international standardization. He is the chairman of IEC Technical Committee 2 Rotating Electrical Machines.